

Supporting Information

Hydrogen bonding enhanced SiO₂/PEO composite electrolytes for solid-state lithium batteries

Cheng Wang, Tianqi Yang, Wenkui Zhang*, Hui Huang, Yongping Gan, Yang Xia, Xinping He and Jun Zhang*

College of Materials Science and Engineering, Zhejiang University of Technology, Hangzhou 310014, China.

E-mail: zhangjun@zjut.edu.cn; msechem@zjut.edu.cn

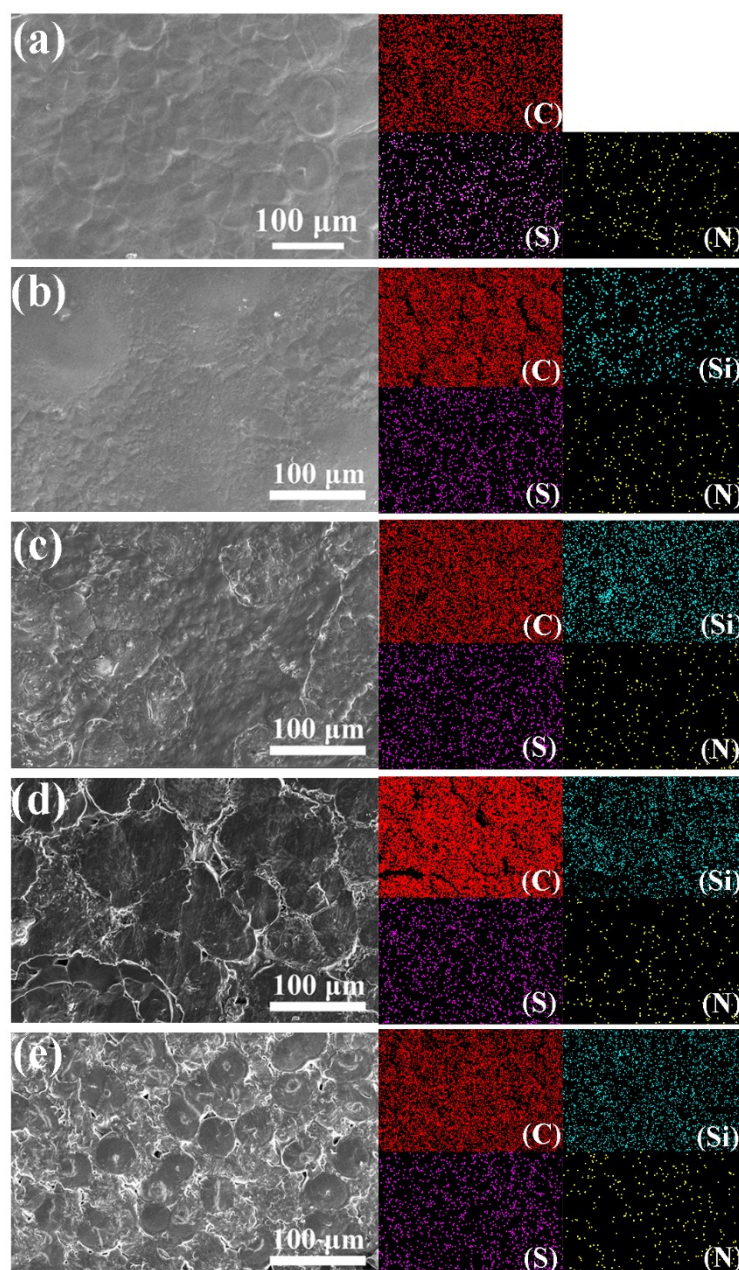


Fig. S1. The SEM images and EDS elemental mappings of 0E (a), 10E (b), 5I (c), 15I (d) and 20I (e).

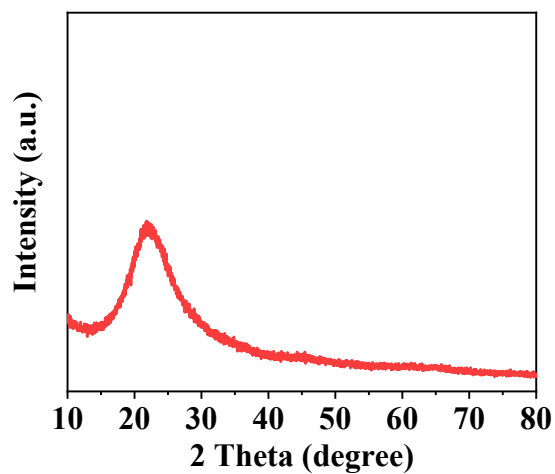


Fig. S2. The XRD patterns of SiO₂ prepared by hydrolysis.

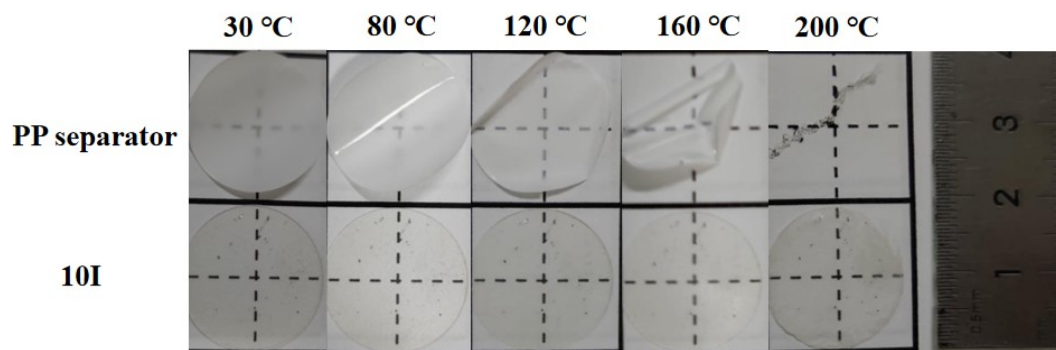


Fig. S3. The optical photos of commercial separator and 10I at different temperatures.

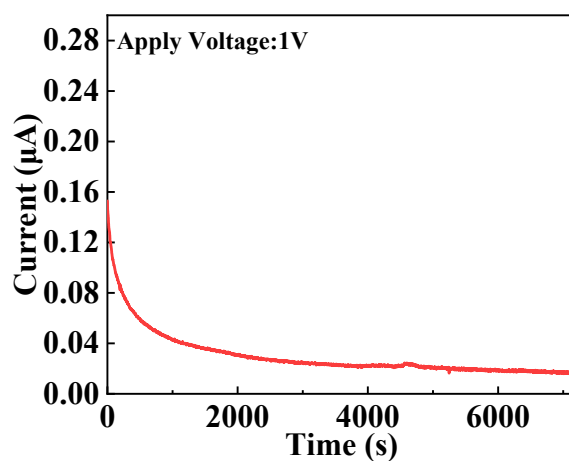


Fig. S4. The time dependent DC current of SS|10I|SS under a constant voltage of 1 V. The electronic conductivity was calculated according to the equation: $\gamma = I_s \cdot l / S \cdot U$, where I_s is the steady-state current obtained in DC polarization measurements, U is the

applied potential (1 V), l is thickness of the solid electrolyte, S is the area of the electrolyte contacted with the SS. The electronic conductivities of SS|10I|SS is calculated to be $2.0 \times 10^{-10} \text{ S cm}^{-1}$.

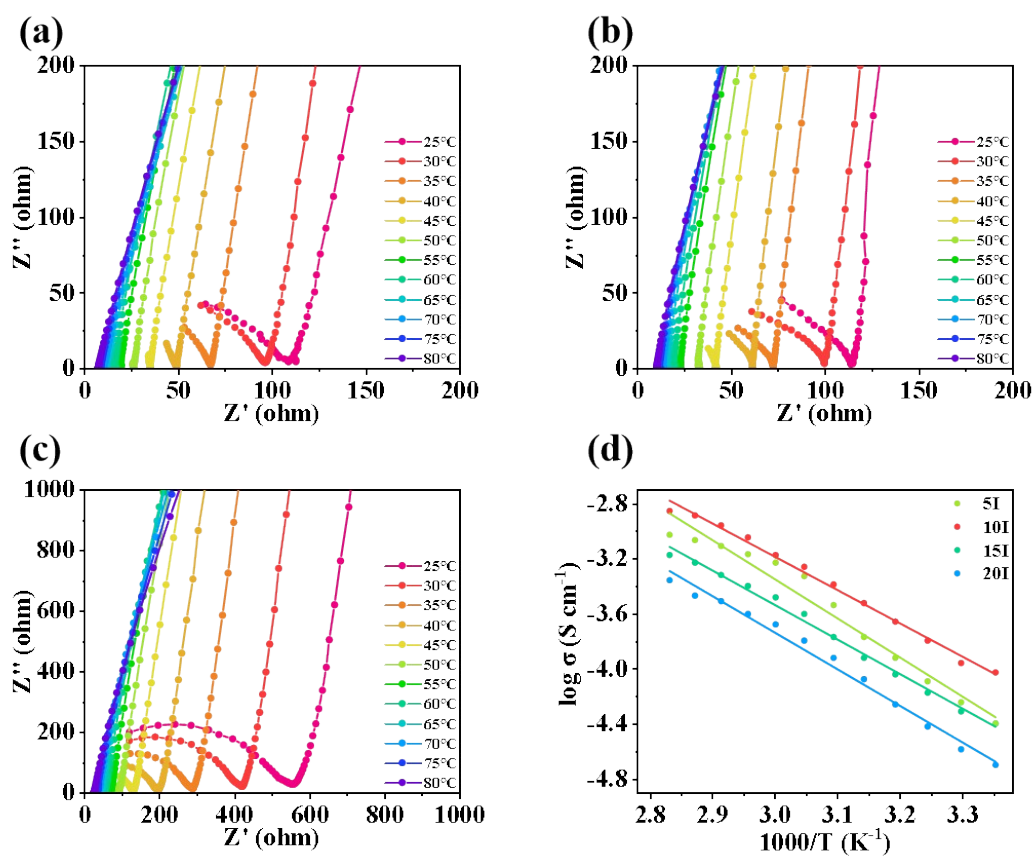


Fig. S5. Nyquist plots of 5I (a), 15I (b) and 20I (c) at different temperatures. (d) Arrhenius plots of the conductivity of 5I, 10I, 15I and 20I.

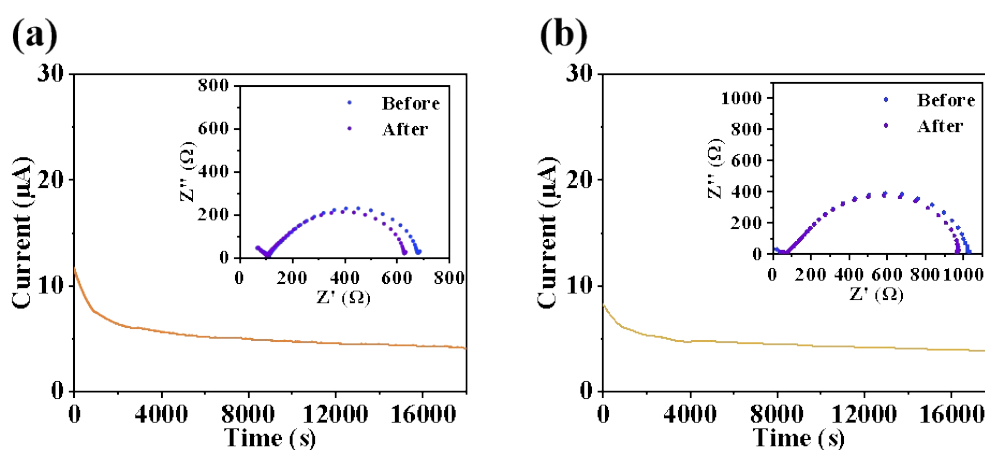


Fig. S6. The chronoamperometry curves of 10E (a) and 0E (b) at a potential step of 10 mV at 30 °C. The inset figure shows the AC impedance spectra of the same cell before and after polarization.

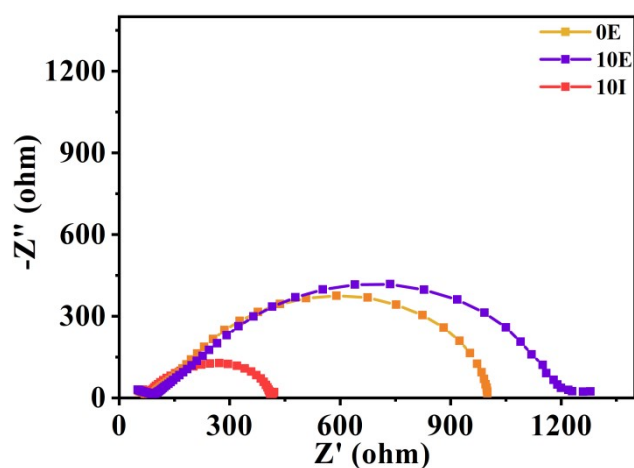


Fig. S7. The impedance spectra of the Li|0E|Li, Li|10E|Li and Li|10I|Li cell.

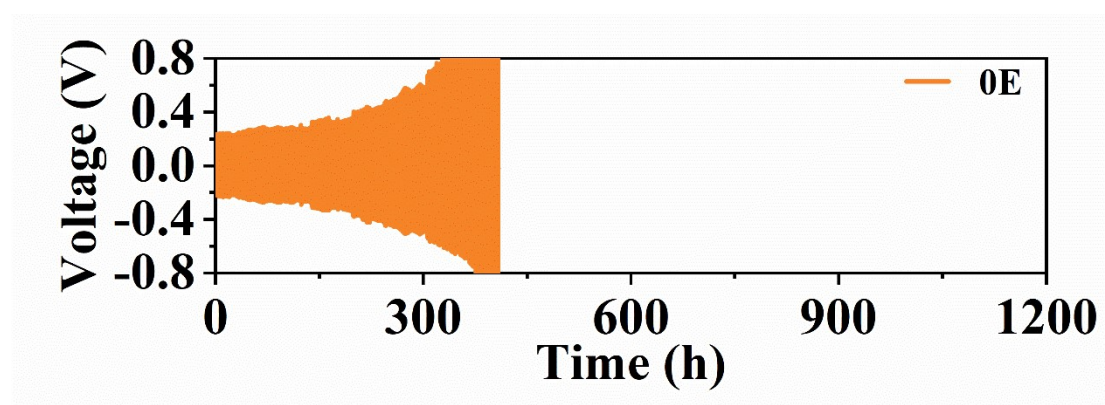


Fig. S8. Voltage profile of the continued lithium plating/stripping cycling of the 10E and 10I battery with a current density of 0.1 mA cm^{-2} at $30 \text{ }^\circ\text{C}$.

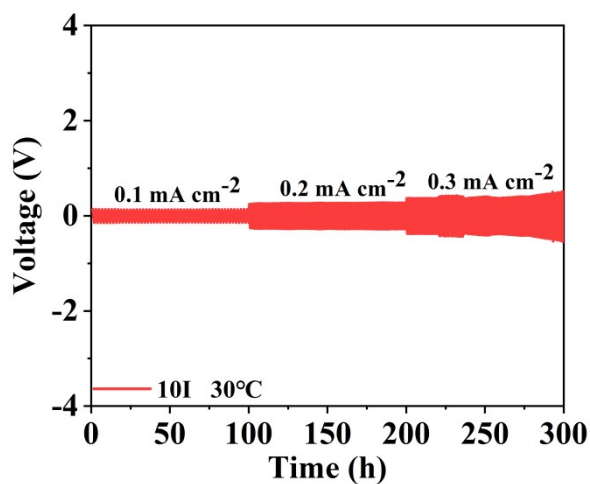


Fig. S9. Voltage profile of the continued lithium plating/stripping cycling of the 10I battery with current density of 0.1 mA cm^{-2} , 0.2 mA cm^{-2} and 0.3 mA cm^{-2} at $30 \text{ }^\circ\text{C}$.

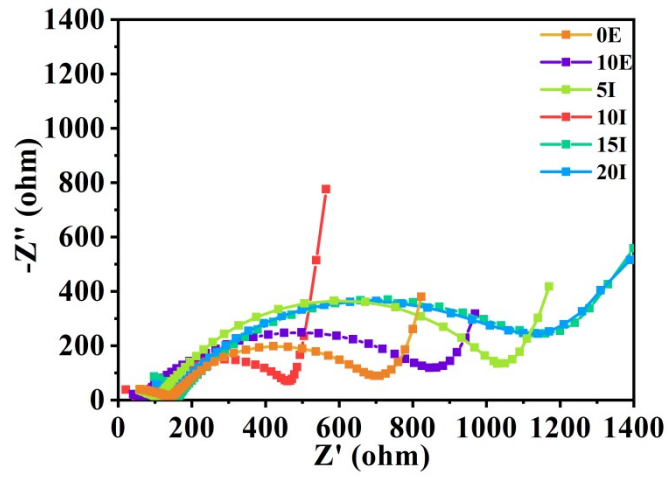


Fig. S10. The impedance spectra of the LFP|0E|Li, LFP|10E|Li, LFP|5I|Li, LFP|10I|Li, LFP|15I|Li and LFP|20I|Li cell.

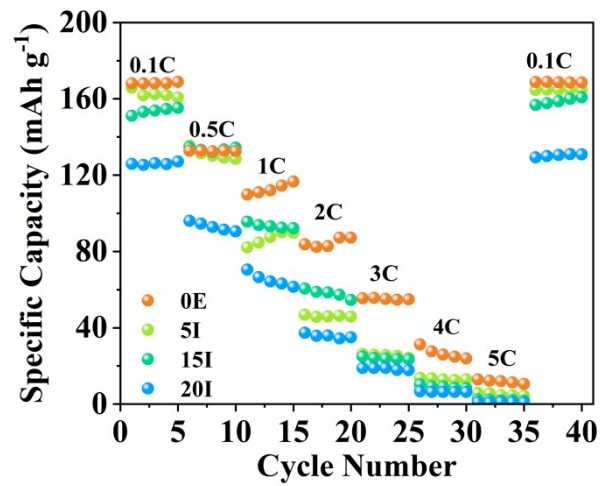


Fig. S11. The rate performances of 0E, 5I, 15I and 20I at 30 °C.

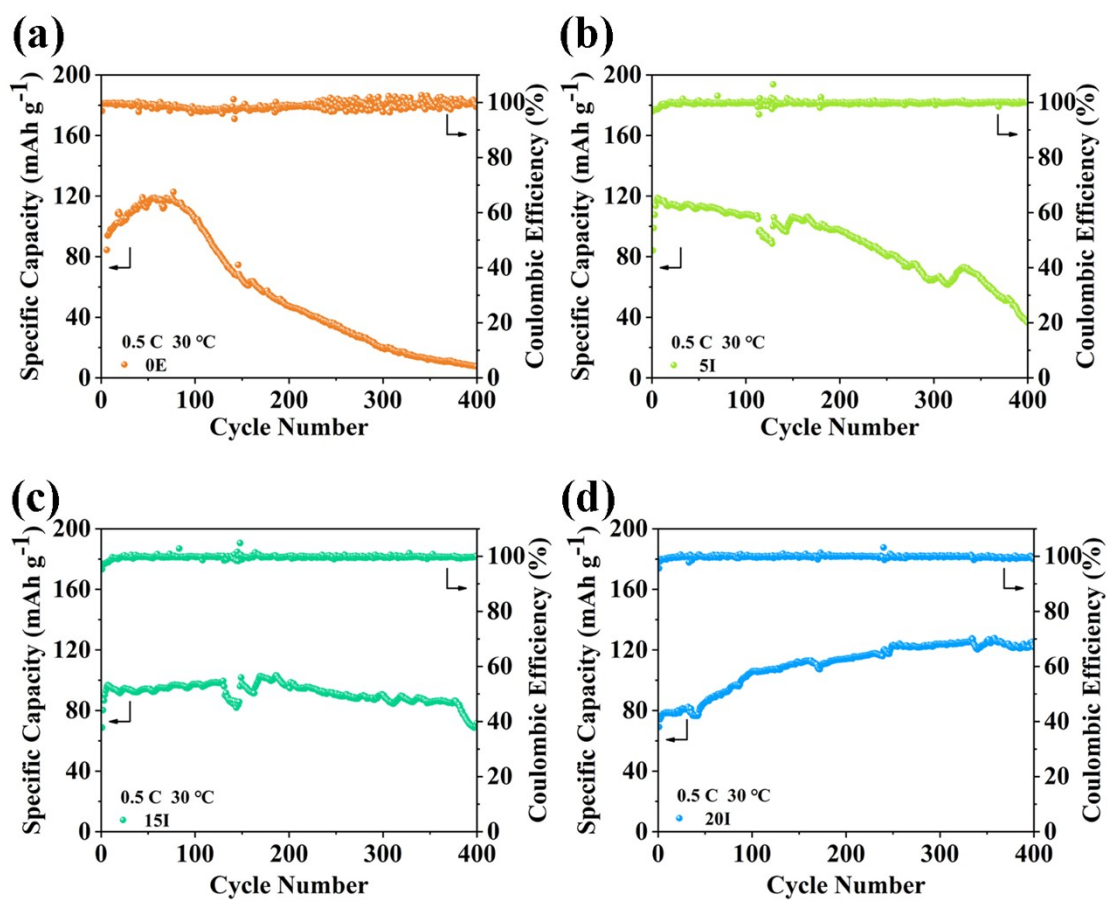


Fig. S12. The cycling performances of 0E (a), 5I (b), 15I (c) and 20I (d) at 0.5C at 30 °C.

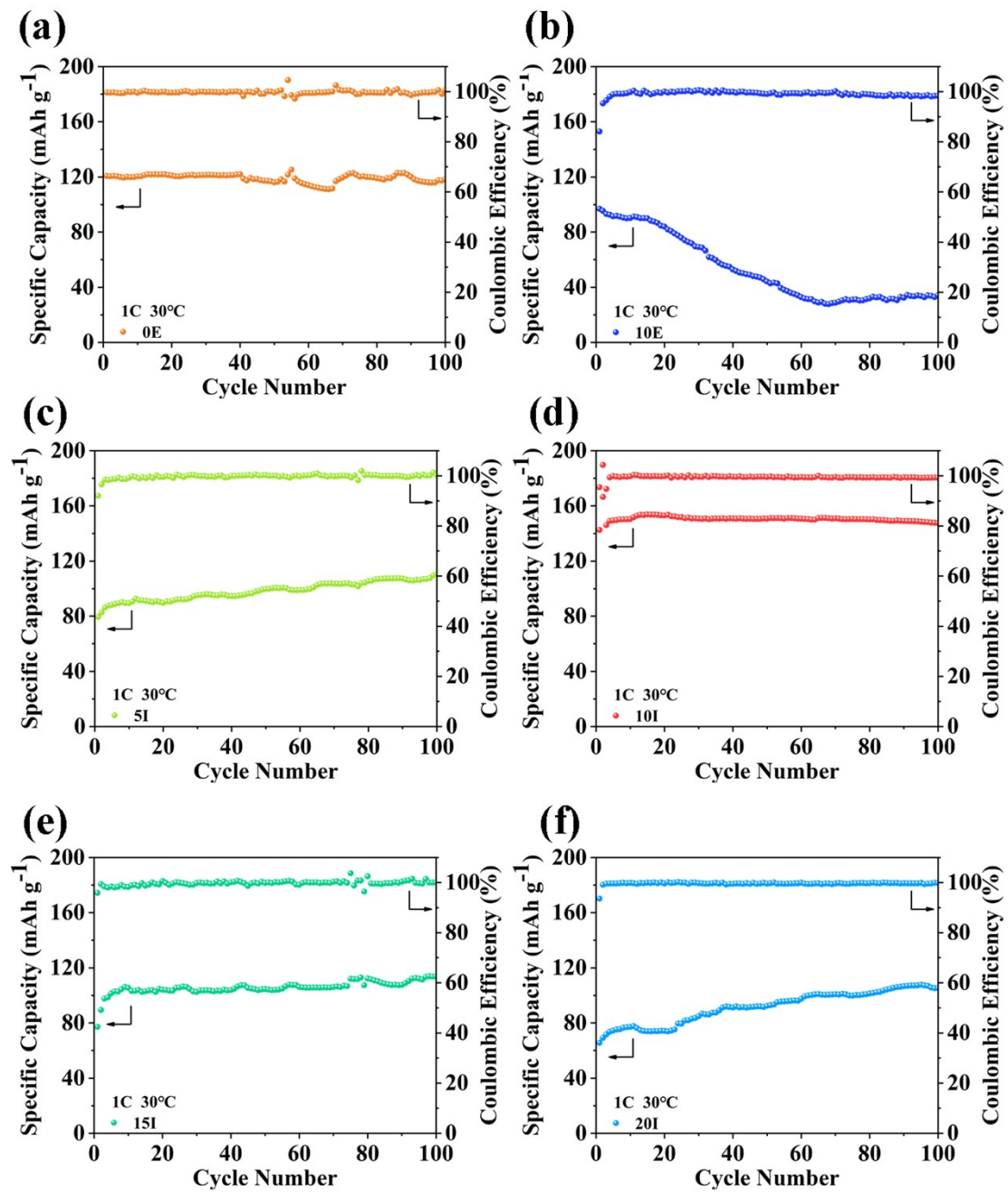


Fig. S13. The cycling performances of 0E (a), 10E (b), 5I (c), 10I (d), 15I (e) and 20I (f) at 1C at 30 °C.

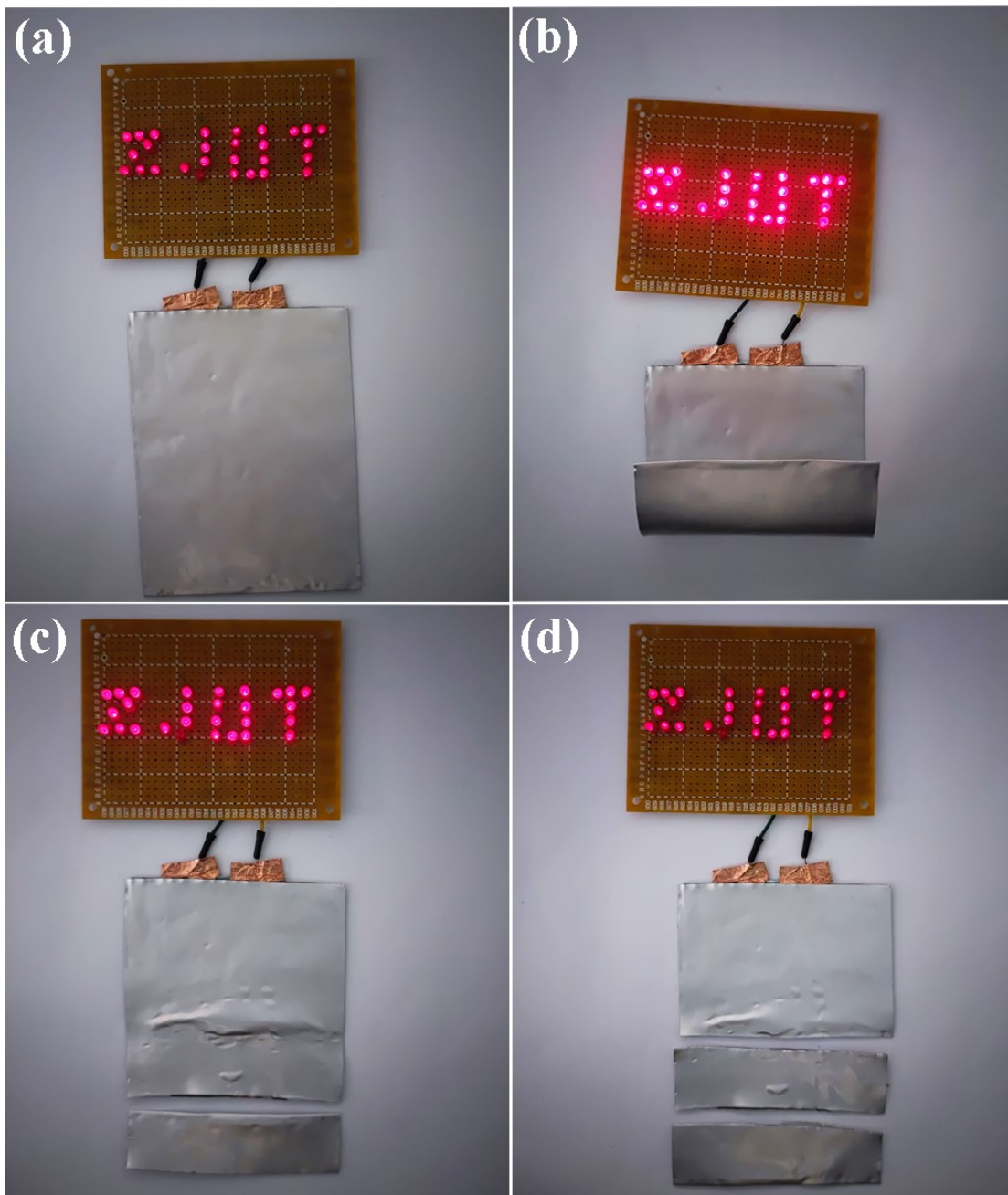


Fig. S14. Optical photos of the LFP/10I/Li pouch cell for the safety performance test at (a) Flat, (b) bending, (c) cut off a quarter, (d) cut off a half.